Applications in Energy and Combustion Science 13 (2023) 100109

Contents lists available at ScienceDirect

Applications in Energy and Combustion Science

journal homepage: www.elsevier.com/locate/jaecs

Optimization of operating conditions of an internal combustion engine used as chemical reactor for methane reforming using ozone as an additive

Pallabi Mishra, Hendrik Gossler, Olaf Deutschmann *

Institute for Chemical Technology and Polymer Chemistry, Karlsruhe Institute of Technology (KIT), Engesserstr. 20, 76131, Karlsruhe, Germany

ARTICLE INFO

Keywords:
Internal combustion engine
Ozone as reaction booster
Numerical optimization
Dry reforming of methane
Hydrocarbon production

ABSTRACT

Internal combustion engines can be used as chemical reactors exploiting the high temperature and pressure as well as short residence time for chemical conversion. For instance, methane and CO_2 can be efficiently converted to H_2 and CO (syngas). The process can be boosted by additives such as dimethyl ether (DME). In this paper, the focus is on optimizing the operating conditions for the use of ozone, O_3, as an alternative fuel additive for dry reforming of methane. Furthermore, methane can be converted to C2 hydrocarbons, which is also studied numerically to find optimized operating conditions, again using O_3 as an additive. The engine is modelled as a single-zone batch reactor under ideal gas assumptions with a variable volume profile. An elementary-step reaction mechanism consisting of 749 reactions among 132 species and including O_3 chemistry was used for the simulations. CO_2 conversion of over 70% is possible using O_3 as an additive, whereas the maximum achievable using DME was around 50%. The optimized yield of C_2H_4 is higher with O_3 as an additive as compared to DME, at all the inlet gas temperatures, whereas it is lower for CH_2O and comparable for C_6H_6 and CH_3OH.

1. Introduction

Internal combustion engines are vastly used in transportation, on land and in water, for more than a century now. Apart from their traditional use as a power source, their potential for alternative applications such as for the production of chemicals, is also being recognized. The first use of the internal combustion engine as a chemical reactor was demonstrated through a patent by Hausser in 1910 for producing nitric oxide and nitric acid [1]. Since then, numerous industries and laboratory research groups have worked on it such as [2–5]. Internal combustion engines have a number of advantages over conventional chemical reactors. They are simple, safe and compact, as well as appropriate temperature and pressure conditions can be reached at very short and defined residence times. They also eliminate the necessity of expensive catalysts, used in conventional reactors, by enhancing reaction speeds through high temperature and pressure conditions possible in them. However, the engine reactors suffer from problems such as the continued need of lubricants, difficulties in controlling the compression ratios as well as scaling up issues, as recently reviewed by Ashok et al. [6].

The reciprocating piston engine can generate very high temperatures up to 1500 K and very high pressures up to hundreds of bars, cyclically, for brief periods in the milliseconds range. The very fast temperature quench allows the reactor to preserve a non-equilibrium state, under which the desired product can be extracted with a good yield. Hence, the engine reactor has been demonstrated for use in the reforming of methane, conversions of methanol, production of nitric acid, nitric oxide and ammonia, the production of sulphur, the production of acetylene, of nanoparticles and of carbon-based nanomaterials [6].

Previous researchers have shown the production of syngas (a mixture of H_2 and CO) in an internal combustion engine such as [7–9]. To initiate the ignition in an internal combustion engine, fuel additives such as dimethyl ether [10], diethyl ether [11] and n-heptane [12] have been used. Though they increase reactivity, large amounts of additives can increase cost and complexity of the process.

Apart from the various carbon-based fuel additives, another candidate for initiating ignition is ozone (O_3) [13–15]. O_3 has the advantage that it forms radicals easily and is thermally stable. It is required in much smaller amounts as compared to DME. While the requirement of DME as a fuel additive is about 5% to 10% of the fuel, O_3 is required in the ppm range, about 10 to 100 ppm [13]. Since proportion of the fuel is more in the inlet gas, it leads to a higher output power of the engine. Moreover, it is possible to generate small quantities of O_3 in inexpensive ozone generators. For example, in one such apparatus demonstrated in [16], 4% v/v O_3 can be produced by passing zero-grade O_2, 99.8% purity, through the inexpensive apparatus constructed using common glassware.

* Corresponding author.
E-mail address: deutschmann@kit.edu (O. Deutschmann).

https://doi.org/10.1016/j.jaecs.2022.100109
Received 1 September 2022; Received in revised form 20 November 2022; Accepted 9 December 2022
Available online 19 December 2022

In the work in [17], an internal combustion engine is used as a chemical reactor using dimethyl ether (DME) as a fuel additive (10% of the fuel, methane) to produce syngas through dry reforming. Numerical optimization was used to find out suitable operating points to maximize the CO_2 conversion and a Rapid Compression Machine (RCM) setup was used to experimentally validate the simulated data.

The outlet gas of the dry reforming simulations described above also has other commercially valuable hydrocarbons in minute quantities. Optimizing the operating for maximizing the mole fractions of these hydrocarbons in the outlet gas looks interesting since these are important raw materials in the chemical industries.

This article investigates CO_2 reforming using O_3 as an alternate fuel additive to overcome the disadvantages of using DME as an additive, such as high cost and complexity as well as reducing the proportion of fuel in the inlet gas. Furthermore, it optimizes the operating conditions for the production of commercially important hydrocarbons, using O_3 as an additive, because of their importance in the chemical industries. The optimized results with O_3 as an additive are then compared with those of DME from previous researches.

2. Methodology

The operating parameters in an internal combustion engine can vary greatly, variation of each of which can give vastly different results in terms of the composition of the outlet gas. Important parameters are the composition of the inlet gas, the inlet gas temperature, the wall temperature, the inlet gas pressure, the engine speed, the compression ratio and the various geometrical parameters of the engine such as the bore, stroke and connecting rod length. Since it is practically difficult to decide on an optimum value for each of these parameters on a hit-and-trial basis, it is more practical to numerically optimize these parameters to get the desired results.

For the research in this article, the simulations were carried out using the DETCHEM^{ENGINE} code. DETCHEM is a software package which can be found in [18]. The DETCHEM^{ENGINE} program (referred to as the ENGINE code in this article), which simulates the time-dependent concentration profiles of the various species in a four-stroke engine.

A single-zone batch reactor is simulated under ideal gas assumptions, with a variable volume profile. The model involves the simultaneous solution of a system of differential equations. Two equations describe the temporal change of moles of each species and the temporal change of temperature. Another two equations are the time dependent volume of the reactor and the Ideal Gas Equation. The heat loss through the walls is accounted for by using the Woschni heat transfer model [19]. The details of the modelling used in the ENGINE code can be found in section 2.1 of [17].

The optimizations were done in a code written using MATLAB. This code gives an initial set of inputs for the optimization variables to the ENGINE code, which runs it to generate an output. The MATLAB code further calculates the objective function from the output generated by the ENGINE code. It uses the 'patternsearch' algorithm [20] to maximize the objective function and generates a further set of inputs to be given to the ENGINE code in the next iteration, which again runs it. This cycle continues until the difference between the values of objective function obtained through consecutive iterations falls below a pre-defined tolerance limit.

The 'patternsearch' algorithm was used because it can accommodate non-linear constraints, as was required in the optimization problems in this work. The algorithm works by taking in an initial set of inputs for the optimization variables, supplied by the user. It calculates the objective function at all points differing by one unit (the default mesh size is 1) from the initial point, in the dimension of each variable. It polls for the point at which it obtains the minimum value of the objective function. This point is taken as the new initial point and it then doubles (this default factor can be adjusted) the mesh size and polls for the point where it obtains the minimum value of the objective function. This iteration continues until at a given point, the value of the objective function at the current initial point is lower than all of the neighbours in the mesh. Taking this as the initial point, it halves the mesh size (this default factor can also be adjusted) and then polls in favour of the point in the mesh where the value of the objective function is lowest. This continues until the value of the objective function is lowest as compared to its neighbours in the mesh, or the difference falls below the user-defined (or default) tolerance limit. The values of the variables at this point is the optimized result given by the algorithm.

All simulations were carried out using the PolyMech mechanism version 2.0 developed by S. Porras and co-workers [21], which includes ozone chemistry as well. The mechanism used in the research has 132 species and 749 chemical reactions. This reaction mechanism assembles the reactions related to the methane combustion, DME and O_3 and was experimentally validated in a rapid compression machine and shock tubes. The geometrical parameters used in the simulations are those of a Volvo TD100 truck engine with a displacement volume of 1.6 litres, compression ratio of 12, a bore of 120.65 mm, a stroke of 140 mm and a connecting rod length of 260 mm. The input variables and the range of parameters were different for the dry reforming and for the production of hydrocarbons. Those have been included in detail in the respective sections (in Section 3 for dry reforming and in Section 4 for the production of hydrocarbons).

3. CO_2 reforming in an internal combustion engine

CO_2 reforming (or dry reforming) involves the endothermic reaction between CO_2 and CH_4 to produce commercially valuable syngas. Dry reforming hence represents a useful method for reducing CO_2 emissions from vehicles or industries [22]. This chemical reaction is given by the following equation:

$$\begin{aligned} CH_4 + CO_2 &\longrightarrow 2CO + 2H_2 \\ \Delta H^r &= 247 \text{ kJ mol}^{-1} \end{aligned} \tag{1}$$

The research in [17] describes the numerical optimization of the operating conditions for maximizing CO_2 conversion in an internal combustion engine using DME as the fuel additive and serves as a baseline for comparison against O_3. This section here aims at studying the optimization of the operating conditions using O_3 as an additive instead and then comparing the results with those obtained using DME as the fuel additive.

This section compares the CO_2 conversion using O_3 and DME as fuel additives. The optimized mole fractions of inlet gases, using DME as an additive, were taken from [17], in which the fuel was taken as 90% CH_4 and 10% DME. The same mole fractions of inlet gases were simulated under the operating conditions (inlet temperature, wall temperature, inlet pressure, engine speed, compression ratio and geometrical parameters) in which the optimizations were carried out for maximizing CO_2 conversion using O_3 as the additive. The results were then compared to the optimized results obtained using DME. The optimizer takes in CO_2 conversion as the objective function to be maximized, which is given by

$$X_{CO_2} = 1 - \frac{n_{CO_2}(t)}{n_{CO_2}(t_0)} \tag{2}$$

Here $n_{CO_2}(t)$ is the number of moles of CO_2 at the end of the cycle and $n_{CO_2}(t_0)$ is the number of moles of CO_2 at the beginning of the cycle.

The mole fraction of O_3 is kept at less than 4% relative to CH_4. This constraint was chosen taking into consideration the maximum capacity of commercially available ozone generators. Argon was added in [17] because the analytics in the experiments required a small amount of the gas to be present, and the lower bound during the optimizations was kept at 2%. Since this research compares O_3 as a fuel additive against DME, Argon is used here and with the same lower bound.

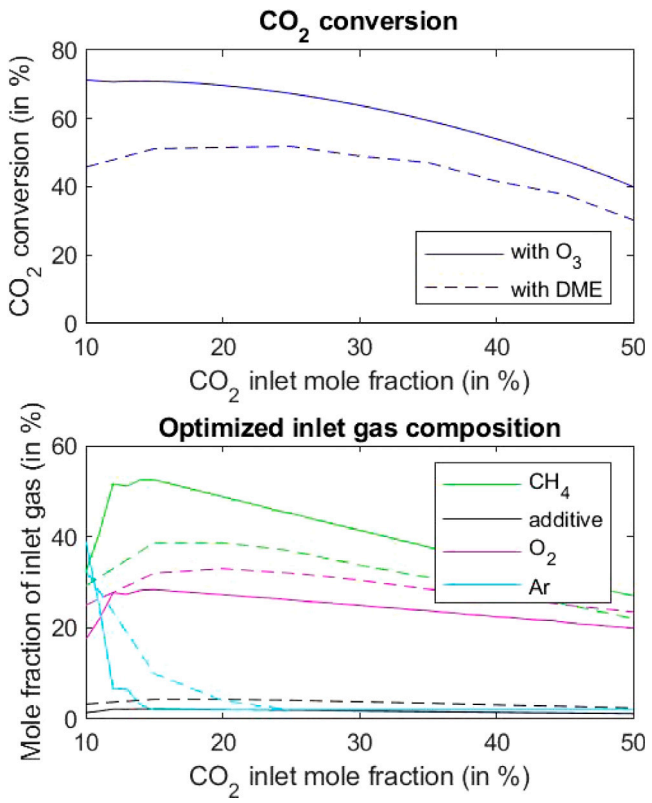

Fig. 1. Optimization of CO_2 dry reforming using O_3 as an additive. The top graph shows the CO_2 conversions using O_3 (solid lines) and DME (dashed lines) as additives. The bottom graph shows the optimized mole fraction of each inlet gas, with O_3 (solid lines) and DME (dashed lines) as additives.

The optimization variables are the individual compositions of the inlet gas, i.e., the inlet mole fractions of CH_4, O_2, O_3 and Ar. The other parameters are kept constant for the optimizations, the inlet temperature at 650 K, the wall temperature at 450 K, the inlet pressure at 1 atm, the engine speed at 60 s^{-1} (3600 rpm) and the compression ratio at 12. The optimization is carried out for different inlet mole fractions of CO_2, from 10% to 50%, varying in the steps of 5% each. The CO_2 conversions for the optimized operating conditions are shown in Fig. 1. As seen in the figure, the CO_2 conversion reduces gradually from about 70% to about 40% with increasing CO_2 inlet mole fractions.

The optimizations have been done for nine different inlet mole fractions of CO_2 (10% to 50% inlet mole fraction of CO_2 in the steps of 5% each). Each optimization results in the optimized inlet mole fraction of four gases (CO_2, additive, O_2 and Argon). Hence, the optimized mole fractions of the individual components in the inlet gas are only graphically shown in the bottom graph of Fig. 1. As can be seen in the figure, the optimized mole fractions of CH_4 and O_2 increase with increasing CO_2 inlet mole fraction from about 30% to 50% and 20% to 30% respectively, for up to the CO_2 mole fraction of 15%, and then gradually decrease to 30% and 20% respectively. The optimized mole fraction of Ar decreases from about 40% to 2% which is the lower bound, up to the CO_2 mole fraction of 15% and then stays at the lower bound. The optimized mole fraction of O_3 stays at the maximum allowed 4% of CH_4 for all the CO_2 mole fractions. This points to the fact that CO_2 conversion is limited by the allowed mole fraction of O_3 at all the inlet mole fractions of CO_2.

Fig. 1 also shows the CO_2 conversions as well as the optimized mole fractions of the inlet gases DME as the fuel additive. In the case of DME, the CO_2 conversions rise from about 45% to 50% up to the CO_2 inlet mole fraction of 25% and then gradually drop down to about 30%. However, in the case of O_3 as the fuel additive, the CO_2 conversions drop gradually from about 70% to 40% with increasing CO_2 inlet mole fractions. As shown in the figure, the CO_2 conversions are higher for all the inlet mole fractions of CO_2 using O_3 as an additive as compared to DME. In the figure, the optimized gas compositions can also be seen while using O_3 (solid lines) and DME (dashed lines) as additives. The inlet mole fraction of CH_4 is more while using O_3 as an additive than with DME. In case of O_3 as an additive, the mole fraction of CH_4 rises from about 35% to 55% around the CO_2 inlet mole fraction of 15% and then gradually falls back to about 30%, whereas in case of DME as an additive, it increases from about 30% to 40% at the CO_2 mole fraction of 15% before falling down to about 30%. This means greater proportion of fuel is permitted under optimized conditions with O_3 as an additive. The inlet mole fraction of O_2 is seen to be lower with O_3 as an additive (varying between about 20% and 25%) than DME (varying between about 25% to 30%), for all the CO_2 inlet mole fractions. Since the proportion of allowed additives were fixed differently in the constraints while defining the optimization problem, the mole fraction of O_3 is lower than the mole fraction of DME in the respective optimized mixtures for each of the CO_2 inlet mole fractions investigated here.

3.1. Summary

The mole fractions of inlet gases were optimized to maximize the CO_2 conversion at the constant temperature of 462 K and pressure of 1 bar (the conditions were chosen for comparison with the previous results using DME), at different CO_2 inlet mole fractions from 10% to 50%. It was seen that the highest (more than 70%) CO_2 conversion occurs at 10% inlet mole fraction of CO_2 using O_3 as an additive. The optimized results with O_3 as an additive were then compared with those of DME. The observation was that the CO_2 conversion using O_3 as an additive is higher than DME, for all the inlet mole fractions of CO_2 from 10% to 50%.

4. Production of unsaturated and partially oxidized hydrocarbons

The internal combustion engine can also be used as a chemical reactor to produce specific hydrocarbons under optimized conditions. In this section, the operating conditions are optimized for the production of unsaturated hydrocarbons and partially oxidized hydrocarbons using O_3 as an additive. The unsaturated hydrocarbons being analysed here include C_2H_4 (ethylene) and C_6H_6 (benzene). The partially oxidized hydrocarbons being analysed include CH_2O (formaldehyde) and CH_3OH (methanol). These hydrocarbons were chosen due to the fact that not only are they commercially valuable, but also they were present in minute quantities in the outlet gas while optimizing the operating conditions for dry reforming. It is therefore conceivable that these species can be produced in higher amounts, provided the appropriate conditions are identified. The results are further compared against those using DME as an additive. Unlike the previous section on optimizing for maximizing CO_2 conversions where pure O_2 was used at the inlet, here air as a mixture of 79% N_2 and 21% O_2 is used at the inlet.

While optimizing for the operating conditions, the objective function in each optimization is the final mole fraction of the hydrocarbon at the end of the cycle, which needs to be maximized. The optimization variables are the engine speed, with the lower and upper limits being 1 s^{-1} (60 revolutions per minute) and 100 s^{-1} (6000 revolutions per minute) respectively, as well as the inlet mole fractions of the inlet gases, i.e., CH_4, O_3, N_2 and O_2. The fixed conditions are the wall temperature at 450 K and the inlet pressure at 1 bar. The optimization was done for each on the inlet gas temperatures from 450 K to 750 K, in the steps of 10 K each.

4.1. Constraint on the maximum allowed mole fraction of O_3

In the optimizations for maximizing the production of hydrocarbons, the maximum allowed O_3 in the inlet gas depends upon the capacity of the O_3 generator that is being used. Hence, an upper limit is required on the mole fraction of O_3 in the inlet gas, depending on the capacity of the ozone generator, which is derived in this section.

The approach used here is, first the molar rate of generation of O_3 by the given ozone generator is calculated. Then, the molar rate of air inlet into the engine is calculated. The ratio of the former and the later gives the maximum allowed mole fraction of O_3 in the inlet gas.

Let the ozone generator have the capacity to generate ozone at the mass rate of $\dot{m}_{O_3}$ g/s. The molar mass of ozone is 48 g/mol. Hence, the molar rate of generation of ozone is given by:

$$\dot{n}_{O_3} = \frac{\dot{m}_{O_3}}{48} \text{ mol/s} \tag{3}$$

Next, the molar rate of air inlet into the engine needs to be calculated. In this discussion, the molar inlet rate of the engine is not taken as a pre-defined variable. Rather it is calculated from the other variables such as the temperature, the pressure, the engine speed (an optimization variable in this case) and geometrical parameters such as the displacement volume of the engine.

The displacement volume V_D of a single piston of the TD100 Volvo engine that we are taking in the simulations is known to be $1.6 * 10^{-3}$ m^3. If the engine speed is N revolutions per second, then in a four stroke engine, the volume of inlet gas into the engine piston is:

$$\dot{V} = \frac{N}{2}.V_D \tag{4}$$

The factor 2 in the denominator is due to the fact that the four stroke engine takes in the inlet gas only during the intake stroke, which comes only every alternate cycle.

The number of moles of inlet gas during each intake stroke needs to be calculated. Using the Ideal Gas Equation, $PV = nRT$ (where P is the inlet pressure, R is the universal gas constant, which is 8.314462 J/K and T is the inlet temperature), the number of moles of inlet gas is

$$n = \frac{PV}{RT} \tag{5}$$

Differentiating both sides with respect to time and assuming that only V varies with respect to time, the molar flow rate of inlet gas is

$$\dot{n}_{tot} = \frac{P\dot{V}}{RT} \tag{6}$$

The value of $\dot{V}$ can be substituted from Eq. (4).

Now, equation (3) gives the molar rate of generation of O_3 and Eq. (7) gives the molar flow rate of the inlet gas. To get the maximum possible mole fraction of ozone in the inlet gas, the molar rate of generated ozone at maximum capacity is divided by the molar flow rate of the inlet gas. Dividing Eq. (3) by Eq. (7) gives

$$n = \frac{\dot{n}_{O_3}}{\dot{n}_{tot}} \tag{7}$$

Substituting the values of $\dot{n}_{O_3}$ and $\dot{n}_{tot}$ from Eqs. (3) and (7) respectively, the maximum mole fraction of O_3 in the inlet gas is given by

$$n = \frac{\dot{m}RT}{24NV_DP} \tag{8}$$

The engine speed N is an optimization variable in the optimization problem. Since the maximum allowed mole fraction of ozone is dependent non-linearly on the engine speed, a non-linear constraint has to be defined in this case. The capacity of the ozone generator taken for the following optimizations is 5 g/hr, which is the typical capacity found in the laboratory.

4.2. Production of C_2H_4

In this section, the operating conditions are optimized for maximizing the mole fraction of C_2H_4 at the end of the cycle, using O_3 as an additive. The optimized operating conditions are discussed followed by the optimized results. They are further compared with the optimized results while using DME as the fuel additive.

Fig. 2(a) shows the mole fraction of C_2H_4 at the end of the cycle, which is the objective function of the current optimization, against the inlet gas temperature. As can be seen in the figure, the optimized mole fraction of C_2H_4 increases steadily with the increasing inlet gas temperature, from about 2.7% to 3%, except around 700 K, where it briefly drops and climbs back again. This jump can be explained as a result of the optimization code encountering two different maxima at different inlet gas temperatures, and shifting between them in the middle. It can be noted that the graph is zoomed in to show the variations and that the mole fractions of C_2H_4 are fairly constant throughout the whole temperature range considered.

Fig. 2(b) shows the fuel conversion given by

$$X_{CH_4} = 1 - \frac{n_{CH_4}(t)}{n_{CH_4}(t_0)} \tag{9}$$

against the inlet gas temperature. This parameter is a measure of how much of the fuel (CH_4 in this case) has been used up during the cycle. As can be seen in the figure, the fuel conversion also increases steadily along with increasing inlet gas temperature from about 70% to slightly over 81%, except around 700 K, where it briefly drops before climbing back again. This jump can be explained similar to the jump seen in the previous figure, in the case of the objective function.

Fig. 2(c) shows the C_2H_4 yield given by

$$Y_{C_2H_4} = 2\,\frac{n_{C_2H_4}(t)}{n_{CH_4}(t_0)} \tag{10}$$

against the inlet gas temperature. This parameter calculates the ratio of the maximum C_2H_4 that is produced under the given conditions, to the maximum C_2H_4 that can theoretically be produced from the fuel (CH_4 in this case). As can be seen in the figure, the C_2H_4 yield increases steadily from around 20% to around 23% along with increasing inlet gas temperature, except around 700 K, where it briefly drops before climbing back again. A small drop is also observed between 740 K and 750 K.

4.2.1. Optimization results

While optimizing for the operating conditions in order to obtain the maximum number of moles of C_2H_4, it is seen that the optimized mole fractions of O_3 decreases from about 9 ppm to close to 0 ppm with the increasing inlet gas temperature, as can be seen in Fig. 2(d). This figure also shows the maximum allowed mole fraction of O_3 in the inlet gas as calculated for each of the inlet gas temperature. A jump is marked in the maximum allowed mole fraction of O_3. It is seen that the optimized mole fraction of O_3 is always less than the maximum allowed mole fraction in the inlet gas for all the inlet gas temperatures, which means that the possible production of O_3 by the particular ozone generator assumed in these calculations, is not a limiting condition for the optimization in this case.

Fig. 2(e) shows the optimized fuel–air equivalence ratios for the inlet temperatures from 450 K to 750 K. As seen in the figure, the mixture turns only very slightly rich with temperature, with the equivalence ratio being around 4. The figure also shows the optimized values with DME as an additive for comparison. It is seen that the optimized mixture is richer with O_3 as an additive than with DME (equivalence ratio rising from about 3 to 4 with temperature) for the investigated temperature range.

Fig. 2(f) shows the optimized engine speeds against the inlet gas temperatures. The optimized engine speed stays close to the upper

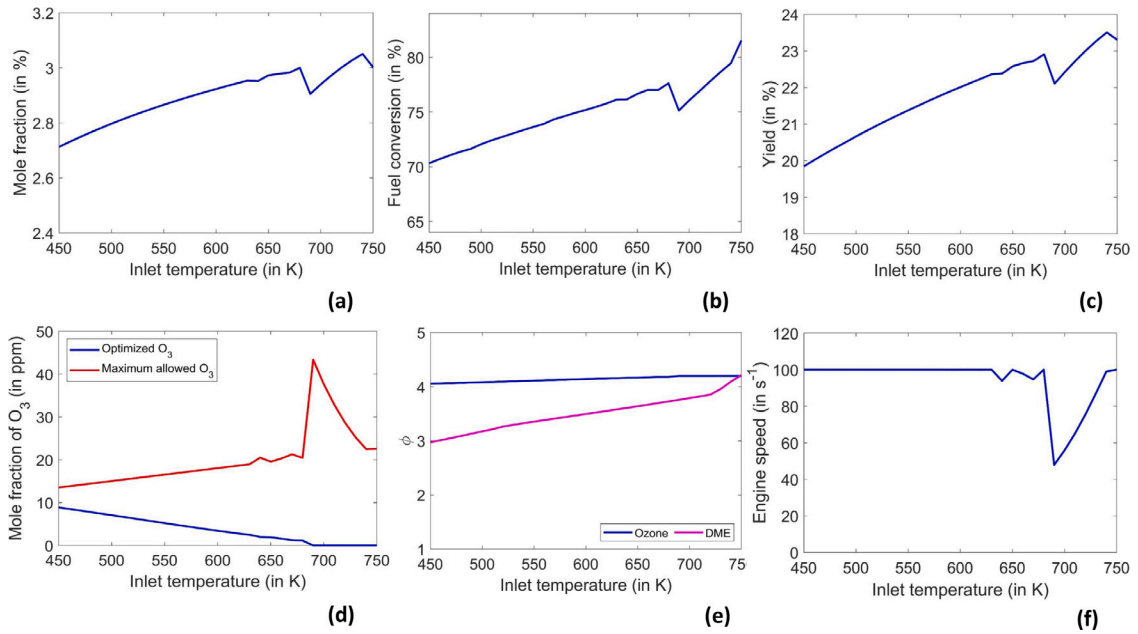

Fig. 2. (a) Optimized C_2H_4 mole fraction (objective function), (b) Fuel conversion, (c) C_2H_4 yield, (d) Optimized mole fraction of O_3, (e) Optimized fuel–air equivalence ratio, and (f) Optimized engine speed, for different inlet gas temperatures from 450 K to 750 K.

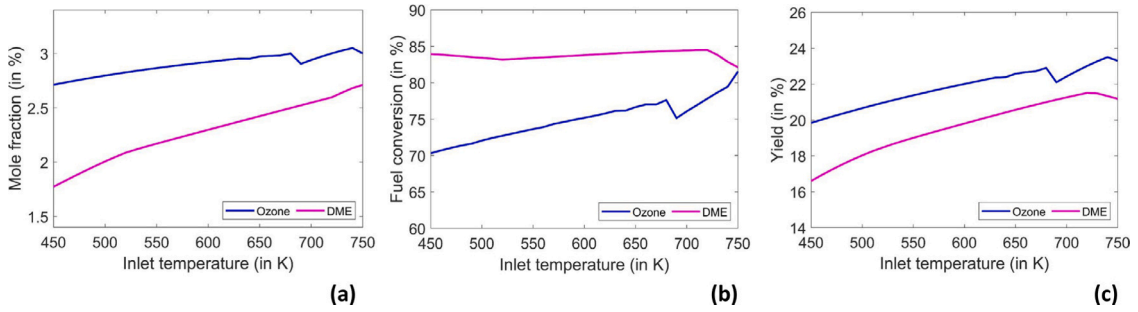

Fig. 3. (a) Optimized C_2H_4 mole fraction (objective function), (b) Fuel conversion, and (c) C_2H_4 yield, for different inlet gas temperatures from 450 K to 750 K, for O_3 and DME as fuel additives.

bound, which is 100 s^{-1} for almost the full range of inlet gas temperature except dropping down and again rising around 700 K. This drop in the optimized engine speed can explain the drop observed in the objective function, in the C_2H_4 yield, as well as in the maximum allowed mole fraction of O_3 in the inlet gas, as seen in the previous figures.

It may be noted here that for brevity, the optimized results do not show the composition of the inlet gases. The individual mole fractions of the inlet gases, for each of the inlet gas temperatures, can however be calculated from the optimized mole fraction of O_3, the optimized fuel–air equivalence ratio and the fact that N_2 and O_2 are present in the inlet gas in the ratio of 79:21. Assuming the individual mole fractions of CH_4, O_2, N_2 and O_3 to be four unknowns, the resulting values of each can be calculated from four equations. The first equation states the optimized mole fraction of O_3. The second equation gives the ratio of the mole fractions of CH_4 and O_2 as given by the optimized fuel–air equivalence ratio. The third equation states the ratio of the mole fractions of N_2 and O_2 to be 79:21. The final equation is formed from the fact that all the individual mole fractions add up to unity.

4.2.2. Comparison against DME as an additive

This section compares the optimized results obtained using O_3 as the fuel additive with those using DME. The mole fraction of DME (as well as other inlet gases) used for comparison was calculated from the optimized data used in [17]. This calculated mole fraction was then simulated with the temperature, pressure and geometrical parameters used for the optimizations done using O_3 as an additive. The same approach for comparison against DME as the fuel additive was used in the sections on the other hydrocarbons as well. Fig. 3(a) shows the mole fraction of C_2H_4, which is the objective function, against the inlet gas temperature, for O_3 as well as DME as fuel additives. As can be seen here, the number of moles of C_2H_4 is higher (rising from about 2.7% to 3% with temperature) while using O_3 as an additive, as compared to DME (rising from 1.8% to 2.5% with temperature), for all the inlet temperatures from 450 K to 750 K.

Fig. 3(b) shows the fuel conversion against the inlet gas temperature using O_3 and DME as additives. The fuel conversion is seen to be lower with O_3 as an additive (rising from about 70% to 81% with temperature) as compared to DME (falling from about 84% to 81% with temperature) at the whole range of inlet gas temperature considered here. Fig. 3(c) shows the C_2H_4 yield against the inlet gas temperature for both O_3 and DME as additives. The yield of C_2H_4 is more with O_3 as an additive (rising from about 20% to 23%) against DME (rising from about 17% to 21%) for the full range of investigated temperatures.

4.3. Production of C_6H_6

In this section, the operating conditions are optimized for maximizing the production of C_6H_6 using O_3 as a fuel additive. The objective function and other parameters are analysed under optimized conditions

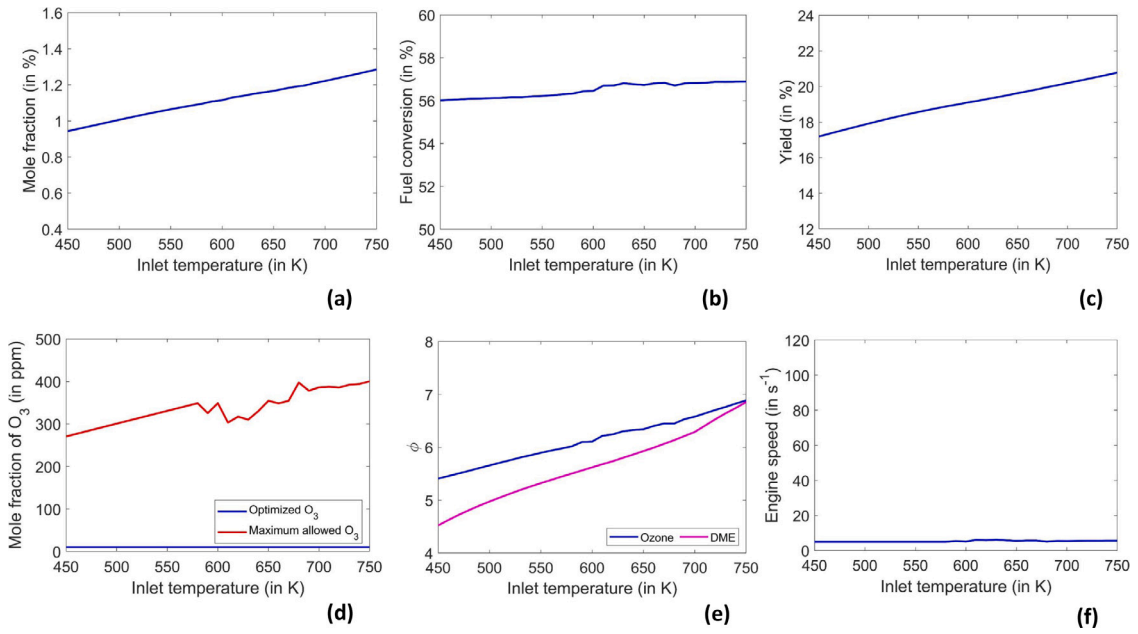

Fig. 4. (a) Optimized C_6H_6 mole fraction (objective function), (b) Fuel conversion, (c) C_6H_6 yield, (d) Optimized mole fraction of O_3, (e) Optimized fuel–air equivalence ratio, and (f) Optimized engine speed, for different inlet gas temperatures from 450 K to 750 K.

and are further compared to those obtained using DME as a fuel additive.

Fig. 4(a) shows the mole fraction of C_6H_6, which is the objective function of the current optimization, against the inlet gas temperature. As can be seen in the figure, the optimized mole fraction of C_6H_6 increases steadily with the increasing inlet gas temperature, from about 0.9% to 1.3%. It may be noted that despite the exaggerated increase projected in the figure, the actual variation is indeed small.

Fig. 4(b) shows the fuel conversion given by Eq. (9) against the inlet gas temperature. As can be seen in the figure, the fuel conversion increases very slightly, remaining around 56%, along with increasing inlet gas temperature.

Fig. 4(c) shows the C_6H_6 yield given by

$$Y_{C_6H_6} = 6\,\frac{n_{C_6H_6}(t)}{n_{CH_4}(t_0)} \tag{11}$$

against the inlet gas temperature. As can be seen in the figure, the C_6H_6 yield increases steadily along with increasing inlet gas temperature, from about 17% to around 21%.

4.3.1. Optimization results

While optimizing the operating conditions in order to obtain the maximum number of moles of C_6H_6, it is seen that the optimized mole fractions of O_3 stays almost constant with the increasing inlet gas temperature, at around 10 ppm, as can be seen in Fig. 4(d). The maximum allowed mole fraction of O_3 in the inlet gas can also be seen in the figure for each of the inlet gas temperature. It is seen that the optimized mole fraction of O_3 is always less than the maximum allowed mole fraction in the inlet gas, which means that the objective function is not bounded by the possible production of O_3 by the ozone generator.

Fig. 4(e) shows the optimized fuel–air equivalence ratios for the inlet temperatures from 450 K to 750 K. As seen in the figure, the optimized mixture becomes richer steadily with temperature, with the equivalence ratio increasing from about 5.5 to 7. Comparing using O_3 as an additive against using DME (equivalence ratio increasing from about 4.5 to 7), it is seen that the optimized mixture is richer with O_3 as an additive for the investigated temperature range.

Fig. 4(f) shows the optimized engine speeds against the inlet gas temperatures. The optimized engine speed stays more or less at the lower bound, which is 5 s^{-1} for almost the full range of inlet gas temperatures.

4.3.2. Comparison against DME as an additive

This section compares the results obtained using O_3 as an additive against those using DME. Fig. 5(a) shows the objective function, the mole fraction of C_6H_6, against the inlet gas temperature, for O_3 as well as DME as additives. As can be seen here, the number of moles of C_6H_6 is slightly higher while using O_3 as an additive (rising from about 1% to 1.3% with temperature), as compared to DME (rising from about 1% to 1.4%), for all the inlet temperatures from 450 K to 750 K.

Fig. 5(b) shows the fuel conversion against the inlet gas temperature for O_3 and DME as additives. As can be seen, the fuel conversion is lesser with O_3 as an additive (around 56%) as compared to DME (falling from about 65% to 60% with temperature). Fig. 5(c) shows the C_6H_6 yield against the inlet gas temperature for both O_3 and DME as additives. The yield of C_6H_6 is less with O_3 as an additive (rising from about 17% to 21% with temperature) as compared to DME (rising from about 21% to 23% with temperature) for the full range of investigated temperatures.

4.4. Production of CH_2O

This section focuses on optimizing the operating conditions for maximizing the mole fractions of CH_2O obtained at the end of the cycle using O_3 as an additive, and then discusses the parameters such as fuel conversion and yield of CH_2O after optimization. It goes on to compare the results with those obtained from using DME as a fuel additive.

Fig. 6(a) shows the mole fraction of CH_2O, which is the objective function of the current optimization, against the inlet gas temperature. As can be seen in the figure, the optimized mole fraction of CH_2O stays almost constant for a short range at around 0.6% before decreasing steadily with the increasing inlet gas temperature up to about 0.2%. Despite the exaggeration seen in the zoomed in figure, the change value of the objective function is very less.

Fig. 6(b) shows the fuel conversion given by Eq. (9) against the inlet gas temperature. As can be seen in the figure, the fuel conversion also decreases along with increasing inlet gas temperature, from about 4% to around 1.5%.

Fig. 6(c) shows the CH_2O yield given by

$$Y_{CH_2O} = \frac{n_{CH_2O}(t)}{n_{CH_4}(t_0)} \tag{12}$$

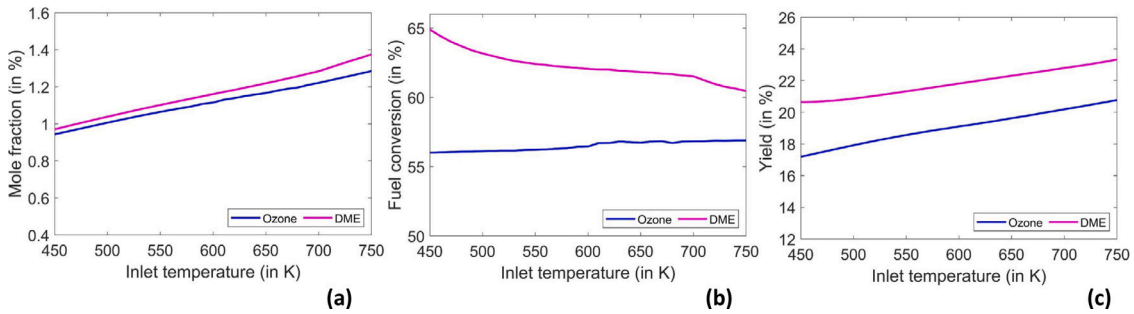

Fig. 5. (a) Optimized C_6H_6 mole fraction (objective function), (b) Fuel conversion, and (c) C_6H_6 yield, for different inlet gas temperatures from 450 K to 750 K, for O_3 and DME as fuel additives.

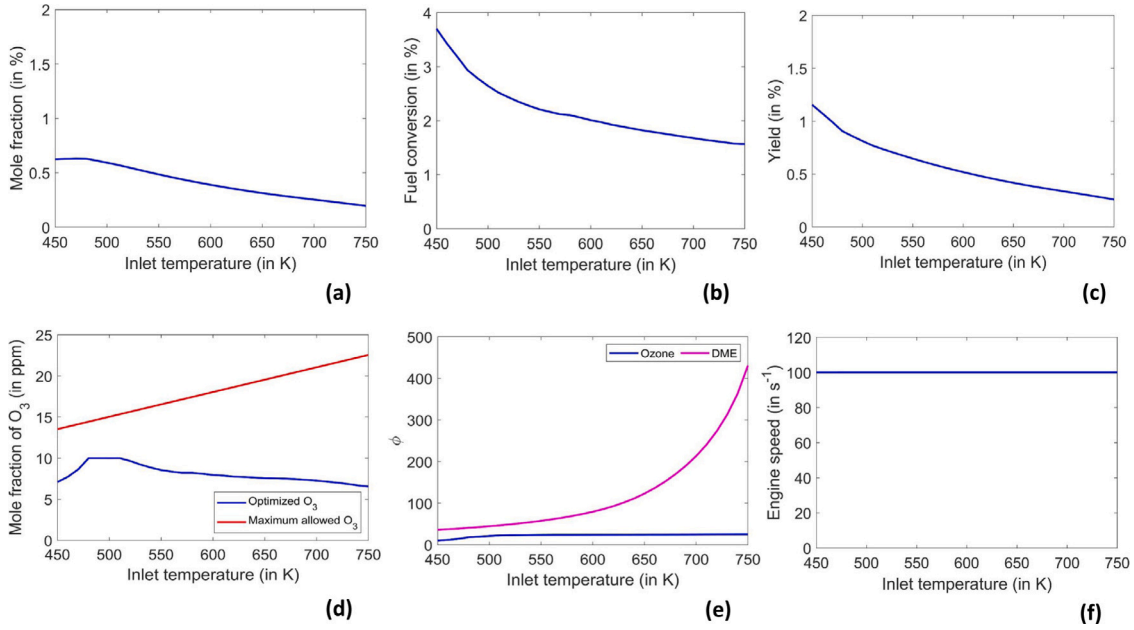

Fig. 6. (a) Optimized CH_2O mole fraction (objective function), (b) Fuel conversion, (c) CH_2O yield, (d) Optimized mole fraction of O_3, (e) Optimized fuel–air equivalence ratio, and (f) Optimized engine speed, for different inlet gas temperatures from 450 K to 750 K.

against the inlet gas temperature. As can be seen in the figure, the CH_2O yield decreases along with increasing inlet gas temperature, from about 1.2% to 0.3%.

4.4.1. Optimization results

The operating conditions were optimized in order to obtain the maximum number of moles of CH_2O at the end of the cycle. It is seen that the optimized mole fractions of O_3 first increases slightly from about 7 ppm to 10 ppm and then steadily decreases with the increasing inlet gas temperature back to about 7 ppm as can be seen in Fig. 6(d). This figure also shows the maximum allowed mole fraction of O_3 in the inlet gas as calculated for each of the inlet gas temperature as well as the optimized engine speed. It is seen that the optimized mole fraction of O_3 is always less than the maximum allowed mole fraction in the inlet gas, which means that it is not bounded by the possible production of O_3 by the ozone generator.

Fig. 6(e) shows the optimized fuel–air equivalence ratio as well as the optimized engine speeds for the inlet temperatures from 450 K to 750 K. As seen in the figure, the optimized mixture becomes rich with temperature, with the equivalence ratio rising from about 10 to 25 with temperature. Comparing using O_3 as an additive against using DME (equivalence ratio rising from about 40 to 430 with temperature), it is seen that the optimized mixture is much leaner with O_3 as an additive for the temperature range considered here.

Fig. 6(f) shows the optimized engine speeds against the inlet temperatures. The optimized engine speed stays very close to the upper bound, which is 100 s^{-1} for the full range of the inlet gas temperature.

4.4.2. Comparison against DME as an additive

In this section, the objective function and the other parameters are compared with O_3 and well as DME under optimized conditions. Fig. 7(a) shows the mole fraction of CH_2O, which is the objective function, against the inlet gas temperature, for O_3 as well as DME as additives. As can be seen here, the number of moles of CH_2O is much lower while using O_3 as an additive (falling from 0.6% to 0.2% with temperature), as compared to DME (rising from about 2.9% to 3.5% with temperature), for all the inlet temperatures from 450 K to 750 K.

Fig. 7(b) shows the fuel conversion against the inlet gas temperature for both O_3 and DME as additives. As can be seen, the fuel conversion is more with O_3 as an additive (falling from about 4% to 2% with temperature) as compared to DME (rising from about 2% to 7% with temperature) at lower temperatures up to about 500 K and lesser at temperatures higher than 500 K. Fig. 7(c) shows the CH_2O yield against the inlet gas temperature for O_3 and DME as additives. The yield of CH_2O is much lesser with O_3 as an additive (falling from 1.2% to 0.3%) as compared to DME (about 3.5%) for the full range of temperatures taken here.

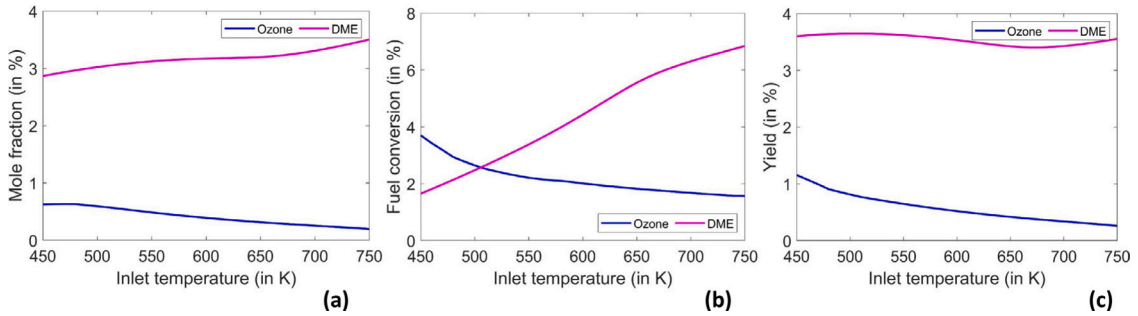

Fig. 7. (a) Optimized CH_2O mole fraction (objective function), (b) Fuel conversion, and (c) CH_2O yield, for different inlet gas temperatures from 450 K to 750 K, for O_3 and DME as fuel additives.

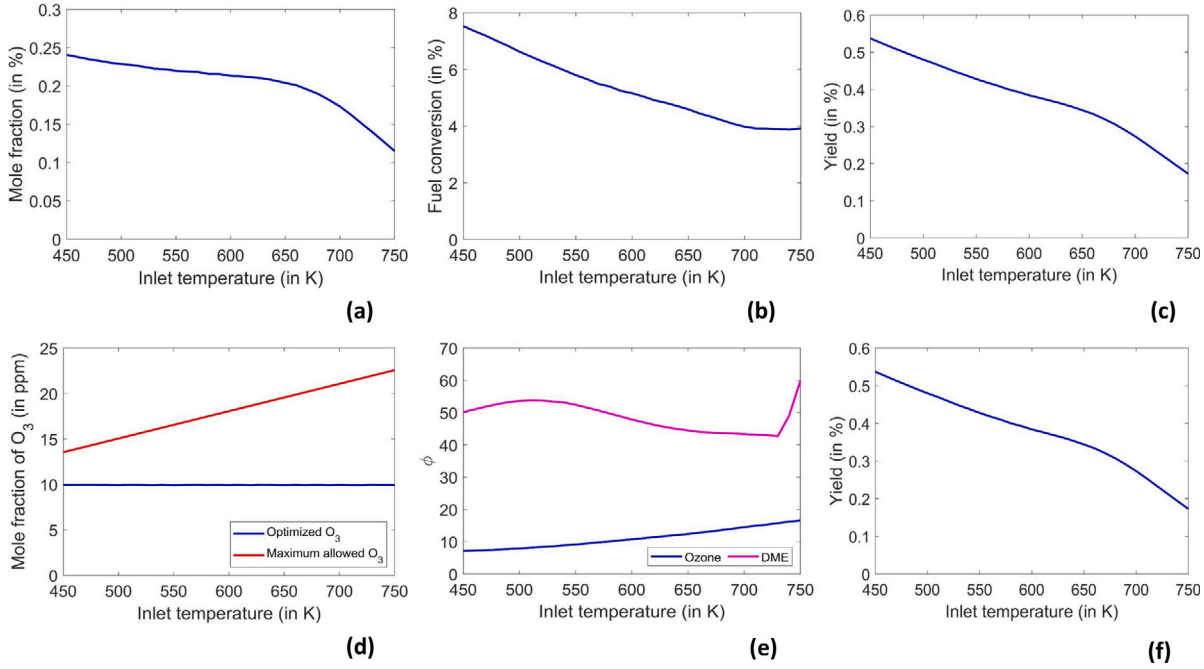

Fig. 8. (a) Optimized CH_3OH mole fraction (objective function), (b) Fuel conversion, (c) CH_3OH yield, (d) Optimized mole fraction of O_3, (e) Optimized fuel–air equivalence ratio, and (f) Optimized engine speed, for different inlet gas temperatures from 450 K to 750 K.

4.5. Production of CH_3OH

This section evaluates the optimization of the operating conditions for maximizing the mole fraction of CH_3OH. Then, it looks at parameters such as the fuel conversion and CH_3OH yield under optimized conditions. Lastly, it compares the optimized results obtained using O_3 and DME as fuel additives.

Fig. 8(a) shows the mole fraction of CH_3OH against the inlet gas temperatures from 450 K to 750 K. As can be seen in the figure, the optimized mole fraction of CH_3OH decreases steadily with the increasing inlet gas temperature, from about 0.25% to 0.1%. It is worthwhile to note here that the large variation with temperature apparent in the figure is indeed a very small change over temperature.

Fig. 8(b) shows the fuel conversion given by Eq. (9) against the inlet gas temperature. As can be seen in the figure, the fuel conversion also decreases steadily along with increasing inlet gas temperature, from about 7.5% to 4%.

Fig. 8(c) shows the CH_3OH yield given by

$$Y_{CH_3OH} = \frac{n_{CH_3OH}(t)}{n_{CH_4}(t_0)} \tag{13}$$

against the inlet gas temperature. As can be seen in the figure, the CH_3OH yield decreases steadily along with increasing inlet gas temperature from about 0.5% to 0.2%.

4.5.1. Optimization results

While optimizing for the operating conditions in order to obtain the maximum number of moles of CH_3OH, it is seen that the optimized mole fractions of O_3 remains nearly constant with the increasing inlet gas temperature as can be seen in Fig. 8(d) at about 10 ppm. This figure also shows the maximum allowed mole fraction of O_3 in the inlet gas as calculated for each of the inlet gas temperatures from 450 K to 750 K. It is seen that the optimized mole fraction of O_3 is always less than the maximum allowed mole fraction in the inlet gas, which means that it is not bounded by the capacity of the ozone generator taken for our optimizations.

Fig. 8(e) shows the optimized fuel–air equivalence ratio as well as the optimized engine speeds for the inlet temperatures from 450 K to 750 K. As seen in the figure, the optimized mixture becomes rich with increasing inlet gas temperature, with equivalence ratio rising from 8 to 16 with temperature. Comparing using O_3 as an additive against using DME (equivalence ratio varying between 42 and 60), it is seen that the optimized mixture is much leaner with O_3 as an additive for the temperature range considered here.

Fig. 8(f) shows the optimized engine speeds against the inlet temperatures. The optimized engine speed very close to the upper bound, which is 100 s^{-1} for almost the full range of inlet gas temperature.

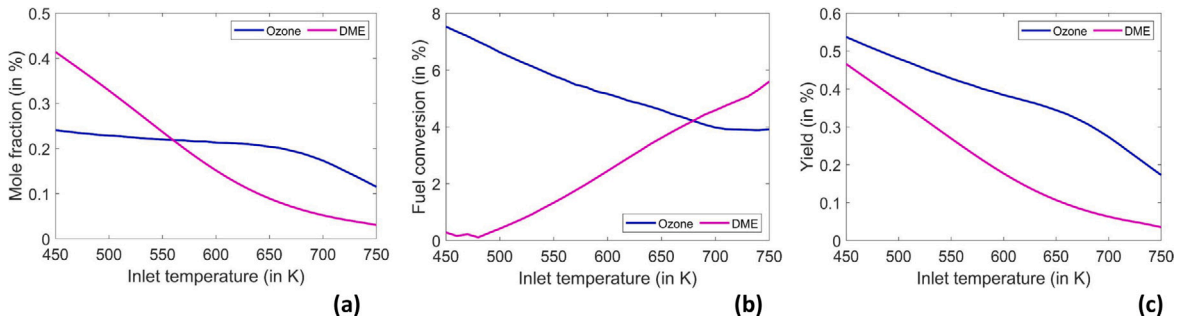

Fig. 9. (a) Optimized CH_3OH mole fraction (objective function), (b) Fuel conversion, and (c) CH_3OH yield, for different inlet gas temperatures from 450 K to 750 K, for O_3 and DME as fuel additives.

4.5.2. Comparison against DME as an additive

This section compares the objective function as well as other parameters using O_3 as an additive against DME. Fig. 9(a) shows the mole fraction of CH_3OH, which is the objective function, against the inlet gas temperature, with both O_3 as well as DME as additives. As can be seen here, the number of moles of CH_3OH is lower while using O_3 as an additive (falling from about 0.25% to 0.1% with temperature), as compared to DME (falling from about 0.4% to about 0.05% with temperature), for the lower inlet temperatures up to around 500 K, whereas it is higher at inlet temperatures above about 500 K.

Fig. 9(b) shows the fuel conversion against the inlet gas temperature for both O_3 and DME as additives. As can be seen, the fuel conversion is more with O_3 as an additive (falling from about 7.5% to 4% with temperature) as compared to DME (rising from 0.2% to about 6% with temperature) at lower temperatures up to about 680 K, and lesser at inlet gas temperatures higher than that. Fig. 9(c) shows the CH_3OH yield against the inlet gas temperature for both O_3 and DME as additives. The yield of CH_3OH is more with O_3 as an additive (falling from about 0.5% to 0.2% with temperature) as compared to DME (falling from about 0.45% to 0.05% with temperature) for the full range of investigated temperatures.

4.6. Summary

In this section, the operating conditions were optimized for maximizing the mole fractions obtained at the end of the cycle, for four hydrocarbons, i.e., C_2H_4, C_6H_6, CH_2O and CH_3OH. The trends in the objective function, the fuel conversion and the yields of the respective hydrocarbons were analysed with respect to the inlet gas temperatures, considered here from 450 K to 750 K, in the steps of 10 K each.

An interesting observation in all the four cases was that the optimized mole fraction of O_3 was always lower than the maximum allowed mole fraction, for the full temperature range considered here, pointing to the fact that the objective function was not limited by the capacity of the ozone generator (5 g/h taken in this case).

While comparing the results using O_3 as an additive against DME, it makes sense to compare the objective function, i.e., the mole fraction of the hydrocarbon at the end of the cycle, as well as the yield, for different hydrocarbons. It was seen that the yield and the final mole fraction were higher for C_2H_4 while using O_3 as an additive while for C_6H_6, they were comparable. For CH_2O, the yield and the final mole fraction were lower using O_3 as the fuel additive, while these parameters were comparable for CH_3OH using both O_3 and DME as fuel additives.

5. Conclusion

In this article, the operating conditions were optimized for the use of an internal combustion engine as a chemical reactor with O_3 as an additive, for dry reforming as well for the production of commercially valuable hydrocarbons, C_2H_4, C_6H_6, CH_2O and CH_3OH. The results were then compared against the optimized conditions with DME as the fuel additive.

In the section on dry reforming, the optimization variables were the mole fractions of CH_4, O_2, O_3 and Ar in the inlet gas, which were optimized for different CO_2 inlet mole fractions from 10% to 50%. It can be seen that reasonable CO_2 conversion takes place to form syngas with O_3 as the fuel additive, around 70% CO_2 conversion taking place at the CO_2 inlet mole fraction of 10% and gradually decreasing with increasing CO_2 mole fraction. The maximum CO_2 conversion possible with DME as the fuel additive was 50%. The optimized results show that CO_2 conversion was higher with O_3 as an additive compared to DME, at all the inlet CO_2 mole fractions from 10% to 50%.

In the section on the production of hydrocarbons, the optimization variables were the inlet mole fractions of the inlet gases, i.e., CH_4, O_2, N_2 and O_3, which were optimized for different inlet gas temperatures from 450 K to 750 K. It was observed that higher yields were obtained for C_2H_4 with O_3 as an additive than DME for all the inlet gas temperatures. The yields for C_6H_6 and CH_3OH are comparable with both O_3 and DME as fuel additives, whereas for CH_2O, the yields are poorer with O_3 as compared to DME.

This article demonstrates the use of O_3 as a fuel additive as well as a comparison with DME. Hence, it may be advantageous to use O_3 as a fuel additive instead of DME for the dry reforming of CO_2 as well as the production of C_2H_4 under optimized conditions.

Even with O_3, the yields are not promising for some of the products and increasing the allowed mole fraction of O_3 does not improve the situation since the upper bound on the allowed O_3 was not the limiting factor in any of the optimizations. Further work can focus on using O_3 along with DME or other fuel additives. In this research, the inlet pressure and the compression ratio have been kept constant. Future work can also focus on optimizing them along with the composition of the inlet gas.

Declaration of competing interest

The authors declare that they have no known competing financial interests or personal relationships that could have appeared to influence the work reported in this paper.

Data availability

Data will be made available on request.

Acknowledgements

Financial support of this work by the Deutsche Forchungsgemeinschaft within the framework of the DFG research unit FOR 1993 “Multi-functional conversion of chemical species and energy, Germany”, project number, 239921130, is gratefully acknowledged. The authors thank omegadot software and consulting GmbH for a cost-free license of DETCHEM.

References

[1] Häusser F. Process of making nitric acid, application filed May 31, 1906. https://patentimages.storage.googleapis.com/20/8c/df/c805bf2fef0be2/US961350.pdf.

[2] Tartakovsky L, Sheintuch M. Fuel reforming in internal combustion engines. Prog Energy Combust Sci 2018;67:88–114. http://dx.doi.org/10.1016/j.pecs.2018.02.003.

[3] Karim GA, Wierzba I. The production of hydrogen through the uncatalyzed partial oxidation of methane in an internal combustion engine. Int J Hydrogen Energy 2008;33(8):2105–10. http://dx.doi.org/10.1016/j.ijhydene.2008.01.051.

[4] Hegner R, Atakan B. A polygeneration process concept for HCCI-engines – Modeling product gas purification and exergy losses. Int J Hydrogen Energy 2017;42(2):1287–97. http://dx.doi.org/10.1016/j.ijhydene.2016.09.050.

[5] Hegner R, Werler M, Schießl R, Maas U, Atakan B. Fuel-rich HCCI engines as chemical reactors for polygeneration: A modeling and experimental study on product species and thermodynamics. Energy & Fuels 2017;31(12):14079–88. http://dx.doi.org/10.1021/acs.energyfuels.7b02150.

[6] Ashok A, Katebah MA, Linke P, Kumar D, Arora D, Fischer K, Jacobs T, Al-Rawashdeh M. Review of piston reactors for the production of chemicals. Rev Chem Eng 2021;000010151520200116. http://dx.doi.org/10.1515/revce-2020-0116.

[7] Gossler H, Deutschmann O. Numerical optimization and reaction flow analysis of syngas production via partial oxidation of natural gas in internal combustion engines. Int J Hydrogen Energy 2015;40(34):11046–58. http://dx.doi.org/10.1016/j.ijhydene.2015.06.125.

[8] Wiemann S, Hegner R, Atakan B, Schulz C, Kaiser SA. Combined production of power and syngas in an internal combustion engine – Experiments and simulations in SI and HCCI mode. Fuel 2018;215:40–5. http://dx.doi.org/10.1016/j.fuel.2017.11.002.

[9] Yang YC, L. MS, Chun YN. The syngas production by partial oxidation using a homogeneous charge compression ignition engine. Fuel Process Technol 2009;90(4):553–7. http://dx.doi.org/10.1016/j.fuproc.2009.01.002.

[10] Green CJ, Cockshutt NA, King L. Dimethyl ether as a methanol ignition improver: Substitution requirements and exhaust emissions impact. SAE Trans 1990;99:982–91, http://www.jstor.org/stable/44580431.

[11] Dhanasekaran C, Mohankumar G. Hydrogen gas in diesel engine using DEE as ignition source. In: Advanced manufacturing research and intelligent applications. Applied mechanics and materials, vol. 591, Trans Tech Publications Ltd; 2014, p. 150–4, www.scientific.net/AMM.591.150.

[12] Çelik M. Analysis of the effect of n-heptane and organic based manganese addition to biodiesel on engine performance and emission characteristics. Energy Rep 2021;7:1672–96. http://dx.doi.org/10.1016/j.egyr.2021.03.024.

[13] Schröder D, Banke K, Kaiser SA, Atakan B. The kinetics of methane ignition in fuel-rich HCCI engines: Dme replacement by ozone. Proc Combust Inst 2021;38(4):5567–74. http://dx.doi.org/10.1016/j.proci.2020.05.046.

[14] Sun W, Gao X, Wu B, Ombrello T. The effect of ozone addition on combustion: Kinetics and dynamics. Prog Energy Combust Sci 2019;73:1–25. http://dx.doi.org/10.1016/j.pecs.2019.02.002.

[15] Alipour M, Ehghaghi MB, Mirsalim M, Ranjbar F. Energy and exergy analysis of the dual-fuel RCCI engine by ozone-assisted combustion of a lean mixture. J Thermal Anal Calorim 2021;143(5):3677–86. http://dx.doi.org/10.1007/s10973-020-09261-2.

[16] Sponholtz DJ, Walters MA, Tung J, BelBruno JJ. A simple and efficient ozone generator. J Chem Educ 1999;76(12):1712. http://dx.doi.org/10.1021/ed076p1712.

[17] Gossler H, Drost S, Porras S, Schießl R, Maas U, Deutschmann O. The internal combustion engine as a CO_2 reformer. Combust Flame 2019;207:186–95, https://www.sciencedirect.com/science/article/pii/S0010218019302445.

[18] Deutschmann O, Tischer S, Kleditzsch S, Janardhanan V, Correa C, Chatterjee D, et al. DETCHEM. 2020, https://www.detchem.com.

[19] Woschni G. A universally applicable equation for the instantaneous heat transfer coefficient in the internal combustion engine. Technical report, SAE technical paper, 1967, https://www.sae.org/publications/technical-papers/content/670931/.

[20] Find minimum of function using pattern search - MATLAB patternsearch - MathWorks Deutschland, https://de.mathworks.com/help/gads/patternsearch.html.

[21] Porras S, Kaczmarek D, Herzler J, Drost S, Werler M, Kasper T, et al. An experimental and modeling study on the reactivity of extremely fuel-rich methane/dimethyl ether mixtures. Combust Flame 2020;212:107–22. http://dx.doi.org/10.1016/j.combustflame.2019.09.036.

[22] Wang S, Lu GQ, Millar GJ. Carbon dioxide reforming of methane to produce synthesis gas over metal-supported catalysts: state of the art. Energy & Fuels 1996;10(4):896–904. http://dx.doi.org/10.1021/ef950227t.